First published March 7, 2012; doi:10.1152/ajprenal.00682.2011.

Disruption of cyclooxygenase-2 prevents downregulation of cortical AQP2 and AQP3 in response to bilateral ureteral obstruction in the mouse

Line Nilsson,[1,2] Kirsten Madsen,[3] Sukru Oguzkan Topcu,[1,2] Boye L. Jensen,[3] Jørgen Frøkiær,[1,2] and Rikke Nørregaard[1,2]

[1]*The Water and Salt Research Centre and* [2]*Institute of Clinical Medicine, University of Aarhus, Aarhus; and* [3]*Cardiovascular and Renal Research, University of Southern Denmark, Odense, Denmark*

Submitted 19 December 2011; accepted in final form 2 March 2012

Nilsson L, Madsen K, Topcu SO, Jensen BL, Frøkiær J, Nørregaard R. Disruption of cyclooxygenase-2 prevents downregulation of cortical AQP2 and AQP3 in response to bilateral ureteral obstruction in the mouse. *Am J Physiol Renal Physiol* 302: F1430–F1439, 2012. First published March 7, 2012; doi:10.1152/ajprenal.00682.2011.—Bilateral ureteral obstruction (BUO) in rats is associated with increased cyclooxygenase type 2 (COX-2) expression, and selective COX-2 inhibition prevents downregulation of aquaporins (AQPs) in response to BUO. It was hypothesized that a murine model would display similar changes in renal COX-2 and AQPs upon BUO and that targeted disruption of COX-2 protects against BUO-induced suppression of collecting duct AQPs. COX-$2^{-/-}$ and wild-type littermates (C57BL/6) were employed to determine COX-1, -2, AQP2, and AQP3 protein abundances and localization after BUO. In a separate series, sham and BUO wild-type mice were treated with a selective COX-2 inhibitor, parecoxib. The COX-2 protein level increased in wild-type mice in response to BUO and was not detectable in COX-$2^{-/-}$. COX-1 protein abundance was increased in sham-operated and BUO mice. Total AQP2 and -3 mRNA and protein levels decreased significantly after BUO in the cortex+outer medulla (C+OM) and inner medulla (IM). The decrease in C+OM AQP2 and -3 levels was attenuated/prevented in COX-$2^{-/-}$ mice, whereas there was no change in the IM. In parallel, inhibition of COX-2 by parecoxib rescued C+OM AQP3 and IM AQP2 protein level in wild-type mice subjected to BUO. In summary, *1*) In C57BL/6 mice, ureteral obstruction increases renal COX-2 expression in interstitial cells and lowers AQP2/-3 abundance and *2*) inhibition of COX-2 activity by targeted disruption or pharmacological blockade attenuates obstruction-induced AQP downregulation. In conclusion, COX-2-derived prostaglandins contribute to downregulation of transcellular water transporters in the collecting duct and likely to postobstruction diureses in the mouse.

COX-2; parecoxib

PREVIOUS STUDIES INDICATE that the cyclooxygenase (COX)-PG pathway may contribute to renal functional changes after ureteral obstruction (1, 16, 28). Two isoforms of COX have been identified, namely, COX-1 and COX-2. It has been demonstrated that 24-h bilateral ureteral obstruction (BUO) enhances PGE_2 production in cortical and medullary tubules of the rat kidney (28), and we have recently demonstrated that COX-2 is the predominant isoform that is responsible for accumulation of PGE_2, $PGF_{2\alpha}$, prostacyclin metabolite 6-keto-$PGF_{1\alpha}$, and thromboxane-2 in rat kidney tissue in response to BUO (18).

It is well established that BUO and release of BUO is associated with a marked decrease in renal aquaporin (AQP) levels and collecting duct water permeability (6, 12, 16). Previously, it was demonstrated that selective COX-2 inhibition prevents downregulation of AQP2 in response to BUO in the inner medulla (IM) (16–18) and restores urine output toward normal in the first hours after release of obstruction in rats (1). The major effect of prostaglandins on water transport appears to be mediated by the binding of PGE_2 to the EP_3 receptor, subsequently inhibiting increased intracellular cAMP, thereby hindering vasopressin-mediated delivery of AQP2 to the plasma membrane in cortical collecting duct principal cells (7, 25). However, a recent study showed that prolonged treatment with a selective EP_4 receptor agonist of a mice model in which the V2 vasopressin receptor (V2R) gene is conditionally deleted prevents downregulation of renal AQP2 levels, probably due to EP_4 receptor-mediated elevation of cAMP levels in kidney collecting duct cells (14). Moreover, Olesen et al. (21) demonstrated that EP_2 and EP_4 agonists increase both AQP2 phosphorylation and trafficking. We have demonstrated that COX-2 knockout mice (COX-$2^{-/-}$) exhibit lower urine concentrating ability despite increased AQP2 and AQP3 abundances (19). Taken together, these contradictory observations on the regulatory impact of prostaglandins on renal aquaporin abundance/water transport prompt investigations into model systems where the contribution from distinct components of the very redundant system can be defined more precisely. Thus, to gain insight into the role of COX-2 in the obstruction-induced renal AQP changes and overcome the inherent challenges associated with drug specificity in pharmacological approaches, we decided to transfer from a rat to a murine model system and employ mice with targeted disruption of COX-2. We hypothesized that complete ureteral obstruction in the mouse leads to increased renal COX-2 expression and COX-2-dependent downregulation of collecting duct AQP2 and AQP3. To address this question, COX-$2^{-/-}$ and wild-type littermate mice on a C57BL/6 background were used for the experiments. The mild developmental renal injury in COX-$2^{-/-}$ on a C57BL/6 background (19, 29) with higher levels of AQP2 and AQP3 was not considered a drawback to test the present hypothesis regarding downregulation of AQPs in response to BUO. Wild-type and COX-$2^{-/-}$ mice were subjected to BUO for 24 h, and renal tissue abundance and localization of COX-2, COX-1, and collecting duct AQP2 and

Address for reprint requests and other correspondence: R. Nørregaard, The Water and Salt Research Center, Institute of Clinical Medicine, Aarhus Univ., Aarhus Univ. Hospital-Skejby, Brendstrupgaardsvej 100, DK-8200 Aarhus N, Denmark (e-mail: rikke.norregaard@ki.au.dk).

-3 were determined. To ensure that observations were caused by abolished COX-2 activity, experiments were repeated in wild-type mice that were treated with the selective COX-2 inhibitor parecoxib during 24-h BUO.

MATERIALS AND METHODS

COX-2$^{-/-}$ Mice

COX-2$^{-/-}$ mice on a mixed 129/C57 background were originally generated by Dinchuk et al. (3). The breeder pairs were obtained from The Jackson Laboratory (Bar Harbor, ME) on a predominant C57BL/6J background. Animals were further backcrossed to the C57BL/6J genetic background for two consecutive generations before they were used for experiments. Mice were housed at The Biomedical Laboratory, University of Southern Denmark and genotyped as previously described (5). All procedures conformed to the Danish National Guidelines for the care and handling of animals and the published guidelines from the National Institutes of Health. The animal protocols were approved by the board of the Institute of Clinical Medicine, Aarhus University, according to the licenses for use of experimental animals issued by the Danish Ministry of Justice.

Experimental Animals

Studies were performed in COX-2$^{-/-}$ and wild-type mice. The animals had free access to a standard rodent diet (Altromin, Lage, Germany) and tap water. During the experiments, animals were kept in individual cages, with a 12:12-h light-dark cycle, a temperature of 21 ± 2°C, and a humidity of 55 ± 2%. Animals were allowed to acclimatize to the cages 3–4 days before surgery. The animals were placed on anesthesia with isoflurane (Abbott Scandinavia), and during the operation the animals were placed on a heating pad to maintain rectal temperature at 37–38°C. Through a midline abdominal incision, both ureters were exposed and then occluded with a silk ligature.

Animals were allocated to the protocols indicated below. Age- and time-matched, sham-operated controls were prepared and were observed in parallel with each BUO group in the following protocols.

Protocol 1. BUO was induced for 24 h in COX-2$^{-/-}$ and wild-type mice (n = 10). The kidneys were prepared for semiquantitative immunoblotting and quantitative PCR (QPCR; n = 6) or for immunohistochemistry (n = 4). Sham-operated controls were prepared in parallel (n = 9), and the kidneys were prepared for semiquantitative immunoblotting and QPCR (n = 6) or for immunohistochemistry (n = 3).

Protocol 2. Prior to surgery, wild-type mice were injected with a selective COX-2 inhibitor, parecoxib (Pfizer), dissolved in saline (5 mg·kg^{-1}·day^{-1}) for 7 days. Injections with saline as a control were conducted in parallel. BUO was induced for 24 h in mice in both parecoxib-treated (n = 5) and saline-treated (n = 6) mice. Sham-operated controls were prepared in parallel in both parecoxib-treated (n = 4) and saline treated (n = 6) mice. The kidneys were prepared for semiquantitative immunoblotting.

Administration of a dose at 5 mg·kg^{-1}·day^{-1} parecoxib was chosen according to a pharmacological profile study of parecoxib (23).

Blood Sampling and Removal of Kidneys

Twenty-four hours after induction of BUO, mice were reanesthetized with isoflurane. Before death, the aortic bifurcation of the mouse was localized, dissected free, and a blood sample was collected for the determination of plasma electrolytes and osmolality. Rapidly, the kidneys were removed and dissected into the cortex and IM. The plasma concentrations of sodium, potassium, creatinine, and urea were measured (Vitros 950, Johnson&Johnson). Finally, the osmolality of the plasma was determined with a vapor pressure osmometer (Osmomat 030, Gonotec, Berlin, Germany).

Isolation of RNA and QPCR

Total RNA was isolated from mouse cortex and IM with a NucleoSpin RNA II mini kit according to the manufacturer's instructions (Macherey-Nagel). RNA was quantitated by spectrophotometry and stored at −80°C. cDNA synthesis was performed on 0.5 μg RNA with an AffinityScript QPCR cDNA synthesis kit (Stratagene).

For QPCR, 100 ng cDNA served as a template for PCR amplification using Brilliant SYBR Green QPCR Master Mix according to the manufacturer's instructions (Stratagene). Serial dilution (1 ng–1 fg/μl) of cDNA was used as a template for generation of a standard curve. Nested primers were used to amplify standards and kidney cDNA samples: COX-2: sense 5′- GCA GCC AGT TGT CAA ACT GC-3′; antisense 5′-CTC GGA AGA GCA TCG CAG AGG-3′; GenBank accession no. NM_011198.2; AQP2: sense 5′-CTT CCT TCG AGC TGC CTT C-3′; antisense 5′-CAT TGT TGT GGA GAG CAT TGA C-3′; GenBank accession no. NM_009699.2; AQP3: sense 5′-TGT GTG TAC TGG CCA TCG TT-3′; antisense 5′-GTT GAC GGC ATA GCC AGA AT-3′; GenBank accession no. AF104416.1; AQP4: sense 5′-GCA TCG CTA AGT CCG TCT TC-3′; antisense 5′-GGG AGG TGT GAC CAG GTA GA-3′; GenBank accession no. U88623; and GAPDH: sense 5′-TAA AGG GCA TCC TGG GCT ACA CT-3′; antisense 5′-TTA CTC CTT GGA GGC CAT GTA GG-3′; GenBank accession no. M32599.1. Standards and unknown samples were amplified in duplicate in 96-well plates, and PCR was performed for 40 cycles consisting of denaturation for 30 s at 95°C followed by annealing and polymerization at 60°C for 1 min. Emitted fluorescence was detected during the annealing/extension step in each cycle. A post-run melting-curve analysis was performed to ensure

Table 1. *Body and kidney weight and plasma biochemical values from sham-operated and BUO wild-type and COX-2$^{-/-}$ mice*

	Sham		BUO	
	Wild-type	COX-2$^{-/-}$	Wild-type	COX-2$^{-/-}$
Body weight, g	21.6 ± 2.4	21.0 ± 1.5	24.2 ± 1.1	21.8 ± 1.2
Kidney weight, mg/g body wt	6.59 ± 0.20	4.99 ± 0.01†	7.94 ± 0.00*	7.03 ± 0.45*
Plasma creatinine, μmol/l	7.3 ± 1.1	14.7 ± 2.4†	234.5 ± 11.4*	266.8 ± 16.3*
Plasma urea, mmol/l	4.9 ± 0.3	24.6 ± 6.5†	68.6 ± 1.8*	86.9 ± 11.0*
Plasma osmolality, mosmol/kgH_2O	317.2 ± 2.9	348.0 ± 12.7†	412.8 ± 13.0*	437.4 ± 17.4*
Plasma potassium, mmol/l	4.5 ± 0.2	5.1 ± 0.4	8.6 ± 0.3*	9.7 ± 0.3*‡
Plasma sodium, mmol/l	142.8 ± 0.9	144.2 ± 2.4	142.1 ± 0.9	140.6 ± 1.0

Values are means ± SE. BUO, bilateral ureteral obstruction; COX, cyclooxygenase. *$P < 0.05$ BUO-operated compared with sham-operated mice. †$P < 0.05$ sham-operated wild-type compared with sham-operated COX-2$^{-/-}$ mice, ‡$P < 0.05$ BUO-operated wild-type compared with BUO-operated COX-2$^{-/-}$ mice.

only one amplification product. Selected samples were subjected to gel electrophoresis to confirm the expected size of the product and only one product.

Membrane Fractionation for Immunoblotting

The tissue [cortex+outer medulla (C+OM) and IM] was homogenized in dissecting buffer (0.3 M sucrose, 25 mM imidazole, 1 mM EDTA, pH 7.2) containing the following protease inhibitors: 8.5 μM leupeptin (serine and cysteine protease inhibitor, Sigma-Aldrich, St. Louis, MO) and 0.4 mM Pefabloc (serine protease inhibitor, Roche). The tissue was homogenized (30 s at 1,250 rpm) by an Ultra-Turrax T8 homogenizer (IKA Labortechnik) and then centrifuged at 4,500 *g* at 4°C for 15 min. Gel samples were prepared from the supernatant in Laemmli sample buffer contain-

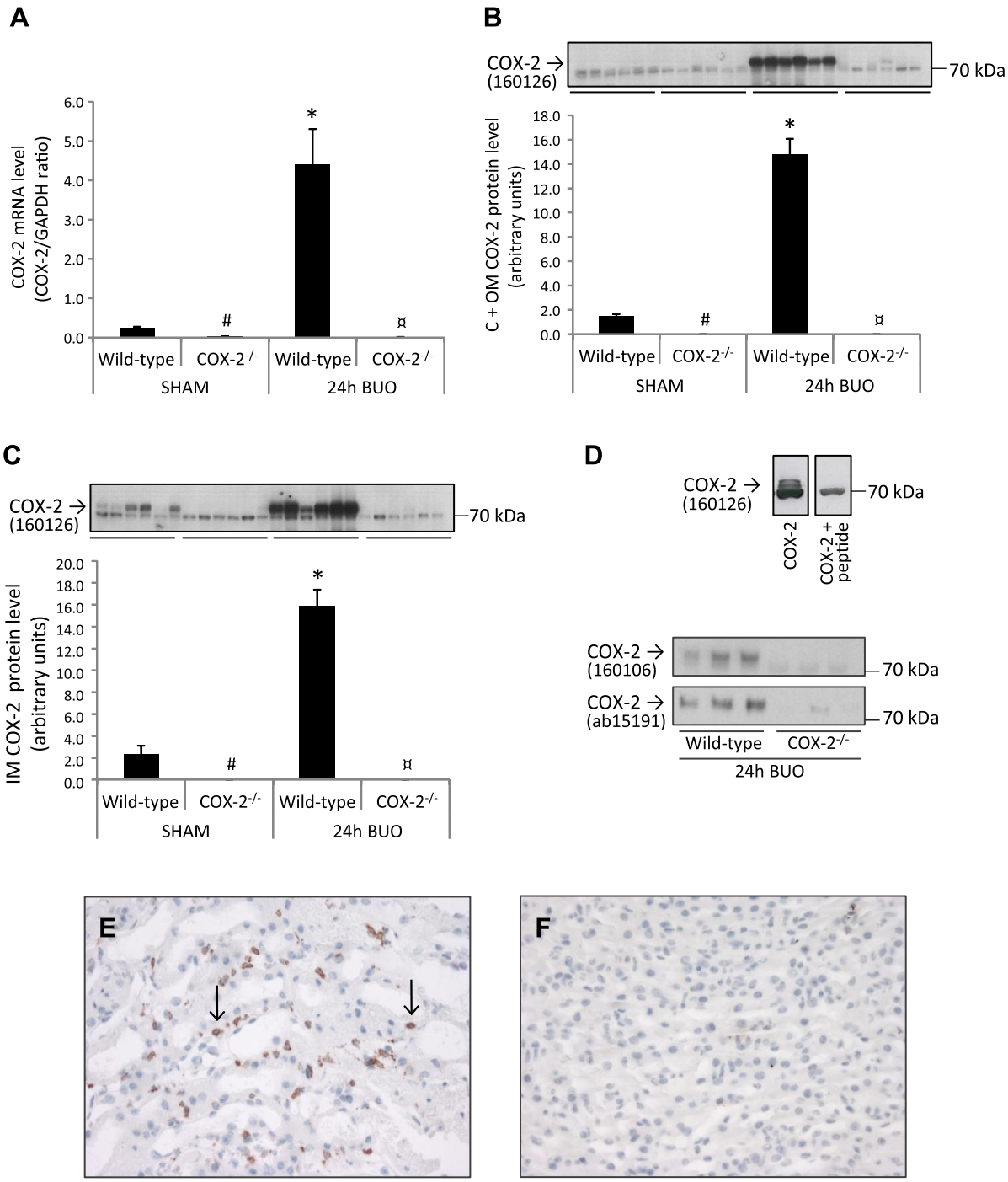

Fig. 1. *A*: cyclooxygenase (COX)-2 mRNA level in cortical and outer medullary (C+OM) kidney tissue. *B*: semiquantitative immunoblots of COX-2 (Cayman 160126) expression in protein isolated from C+OM kidney tissue. *C*: semiquantitative immunoblots of COX-2 (Cayman 160126) expression in protein isolated from inner medullary (IM) kidney tissue. *D*: anti-COX-2 antibody was preincubated with an excess of the immunizing peptide. Semiquantitative immunoblots of COX-2 expression in protein isolated from IM kidney tissue in bilateral ureteral obstruction (BUO)-operated COX-2$^{-/-}$ and wild-type mice probed with an additional 2 COX-2 antibodies: Cayman 160106 and Abcam ab15191. *E*: immunohistochemical staining of COX-2 in IM tissue from BUO-operated wild-type mouse. COX-2 is localized in IM interstitial cells. *F*: immunohistochemical staining of COX-2 in IM tissue from BUO COX-2$^{-/-}$ mice showing no labeling of COX-2.

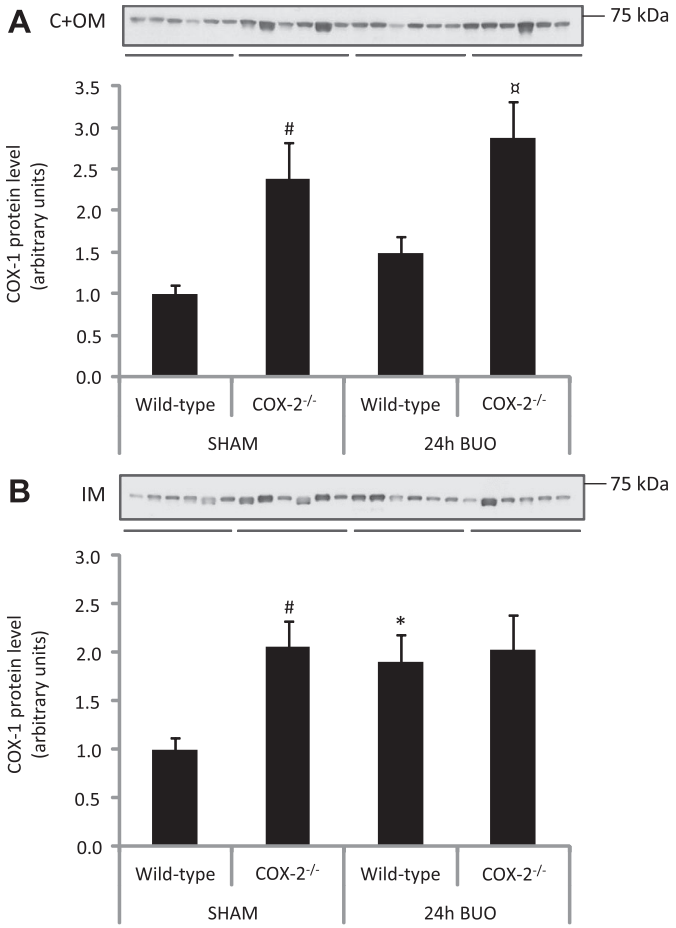

Fig. 2. Effect of BUO on renal regulation of COX-1 protein abundance in COX-2$^{-/-}$ and wild-type mice. *A*: C+OM COX-1 abundance is significantly increased in sham-operated COX-2$^{-/-}$ mice compared with wild-type mice. COX-1 is significantly increased in response to BUO in both wild-type and COX-2$^{-/-}$ mice. *B*: IM COX-1 abundance is significantly increased in sham-operated COX-2$^{-/-}$ compared with sham-operated wild-type mice. IM COX-1 protein abundance is significantly increased in wild-type mice in response to BUO. *$P < 0.05$ BUO-operated compared with sham operated mice. #$P < 0.05$ sham-operated wild-type compared with sham-operated COX-2$^{-/-}$ mice. ¤$P < 0.05$ BUO-operated wild-type compared with BUO-operated COX-2$^{-/-}$ mice.

ing 2% SDS. The total protein concentration of the homogenate was measured using a Pierce BCA protein assay kit (Roche).

Electrophoresis and Immunoblotting

Samples of membrane fractionation from the different zones were run on 12% polyacrylamide minigels (Bio-Rad Mini Protean II). For each gel, an identical gel was run in parallel and subjected to Coomassie staining. The Coomassie-stained gel was applied to determine identical loading or to allow for correction for minor variations in loading.

Samples were run on 12% polyacrylamide gels (Bio-Rad Protean II). Proteins were transferred to a nitrocellulose membrane (Hybond ECL RPN 3032D, Amersham Pharmacia Biotech). Afterward, the blots were blocked with 5% nonfat dry milk in PBS-T (80 mM Na_2HPO_4, 20 mM NaH_2PO_4, 100 mM NaCl, 0.1 Tween 20, adjusted to pH 7.4). After washing in PBS-T, the blots were incubated with primary antibodies overnight at 4°C. The antigen-antibody complex was visualized with horseradish peroxidase (HRP)-conjugated secondary antibodies (P448, diluted 1:3,000, Dako, Glostrup, Denmark) using the enhanced chemiluminescence system (ECL; Amersham Pharmacia Biotech). Immunolabeling controls were performed using peptide-absorbed antibody.

Primary Antibodies

For semiquantitative immunoblotting and immunohistochemistry, we used specific antibodies to renal COX-2 (160126 and 160106, Cayman Chemical, Ann Arbor, MI); COX-2 (ab15191, Abcam, Cam-

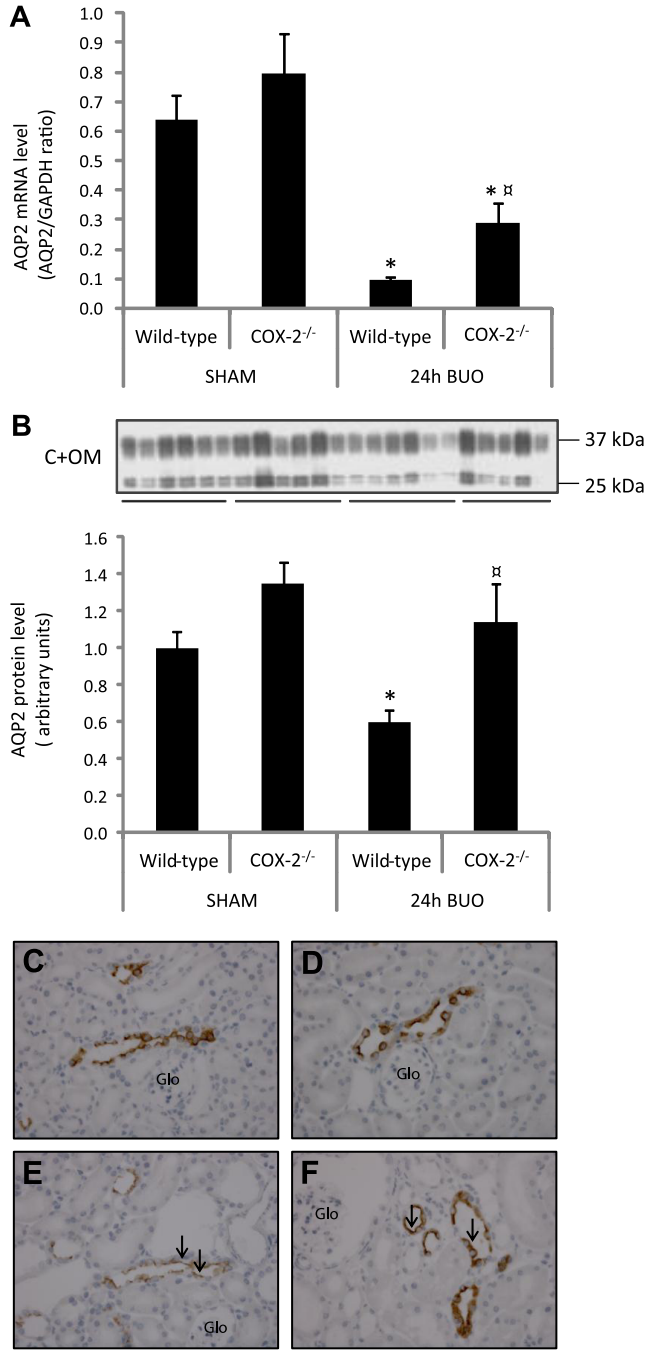

Fig. 3. Effect of BUO on C+OM regulation of aquaporin-2 (AQP2) in COX-2$^{-/-}$ and wild-type mice. *A*: in wild-type mice, C+OM AQP2 mRNA level is significantly decreased as an effect of BUO, but the downregulation is attenuated in COX-2$^{-/-}$ BUO mice. *B*: C+OM AQP2 protein abundance is significantly downregulated in wild-type BUO mice, but the downregulation is absent in COX-2$^{-/-}$ BUO mice. *$P < 0.05$ BUO-operated compared with sham-operated mice. ¤$P < 0.05$ BUO-operated wild-type compared with BUO-operated COX-2$^{-/-}$ mice. *C–F*: cortical immunohistochemical staining of AQP2 showed stronger labeling in COX-2$^{-/-}$ BUO mice compared with wild-type BUO mice. *C*: sham wild-type. *D*: sham COX-2$^{-/-}$. *E*: BUO wild-type. *F*: BUO COX-2$^{-/-}$.

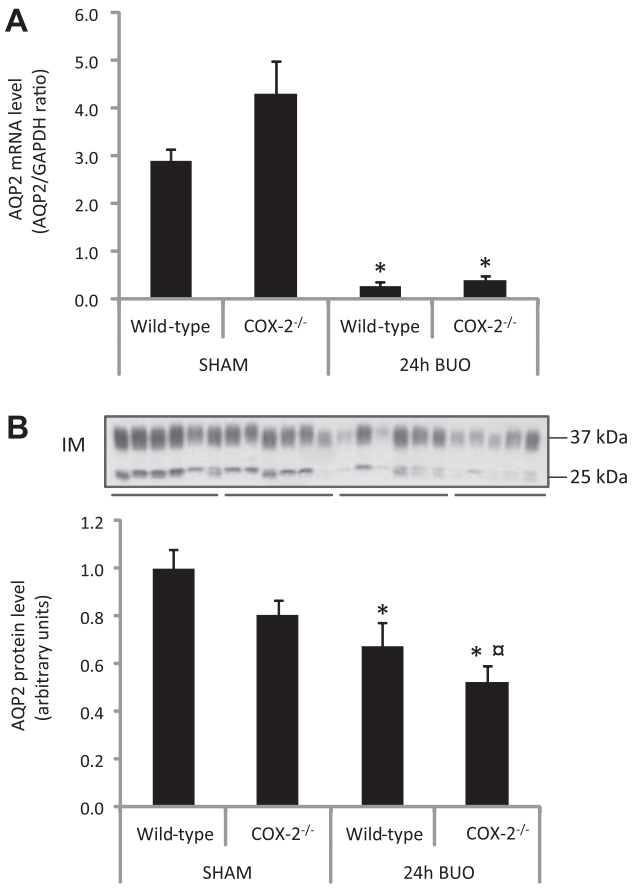

Fig. 4. Effect of BUO on IM regulation of AQP2 in COX-2$^{-/-}$ and wild-type mice. *A*: IM AQP2 mRNA level is significantly decreased in response to BUO in both genotypes. *B*: total IM AQP2 protein abundance showed significant downregulation in response to BUO in both genotypes. *$P < 0.05$ BUO-operated compared with sham-operated mice. ¤$P < 0.05$ BUO-operated wild-type compared with BUO-operated COX-2$^{-/-}$ mice.

bridge, UK); COX-1 (160109, Cayman Chemical); and AQPs, which had been well characterized in previous studies: AQP-2 (H7661) (15), pAQP2Ser256 (KO407) (2), AQP-3 (LL178AP) (4).

Immunohistochemistry

The kidneys from BUO and sham-operated control mice were fixed by retrograde perfusion via the abdominal aorta with 3% paraformaldehyde in 0.1 M cacodylate buffer, pH 7.4. Moreover the kidneys were immersion fixed for 1 h and washed for 3 × 10 min with 0.1 M cacodylate buffer. The kidney blocks were dehydrated and embedded in paraffin. The paraffin-embedded tissues were cut in 2-μm sections on a rotary microtome (Leica Microsystems, Herlev, Denmark).

For immunoperoxidase labeling, the sections were deparaffinated and rehydrated. Endogenous peroxidase activity was blocked with 5% H_2O_2 in absolute methanol for 10 min at room temperature. To expose antigens, kidney sections were boiled in a target retrieval solution (1 mmol/l Tris, pH 9.0, with 0.5 mM EGTA) for 10 min. After cooling, nonspecific binding was prevented by incubating the sections in 50 mM NH_4Cl in PBS for 30 min, followed by blocking in PBS containing 1% BSA, 0.05% saponin, and 0.2% gelatin. Sections were incubated with primary antibodies diluted in PBS with 0.1% BSA and 0.3% Triton X-100 overnight at 4°C. After being washed 3 × 10 min with PBS supplemented with 0.1% BSA, 0.05% saponin, and 0.2% gelatin, the sections were incubated with HRP-conjugated secondary antibody (P448, goat anti-rabbit immunoglobulin, Dako) for 1 h at room temperature. After rinsing with PBS wash buffer, the sites of

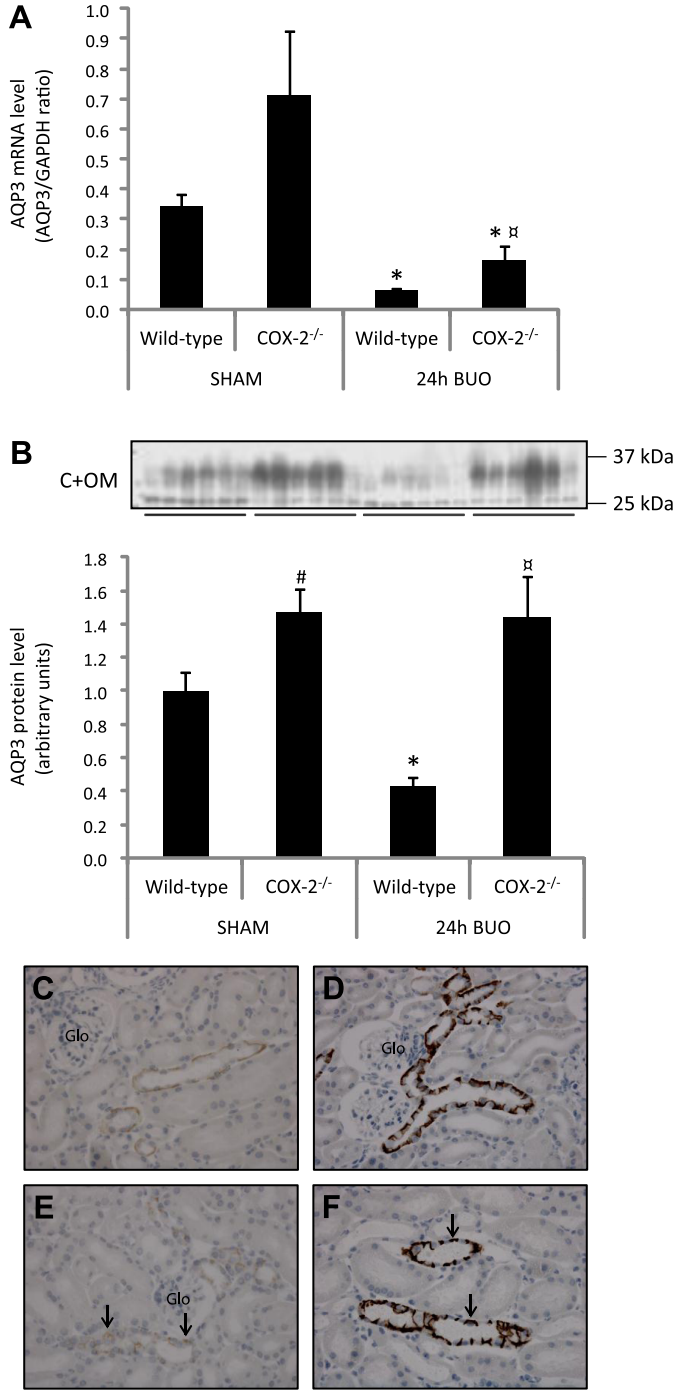

Fig. 5. Effect of BUO on C+OM regulation of AQP3 in COX-2$^{-/-}$ and wild-type mice. *A*: C+OM AQP3 mRNA level is significantly decreased in response to BUO in both genotypes. The downregulation of C+OM AQP3 is attenuated in COX-2$^{-/-}$ mice. *B*: C+OM AQP3 protein abundance is significantly decreased in BUO wild-type mice. The downregulation of C+OM AQP3 is abolished in BUO COX-2$^{-/-}$ mice. *$P < 0.05$ BUO compared with sham-operated mice. #$P < 0.05$ sham-operated wild-type compared with sham-operated COX-2$^{-/-}$ mice. ¤$P < 0.05$ BUO-operated wild-type compared with BUO-operated COX-2$^{-/-}$ mice. *C–F*: cortical immunohistochemical staining of AQP3 showed increased labeling in both COX-2$^{-/-}$ sham-operated and BUO mice compared with wild-type mice. Panels are as described in Fig. 3.

antibody-antigen reactions were visualized with 0.05% 3,3′-diaminobenzidine tetrachloride (Kem-en Tek, Copenhagen, Denmark) dissolved in distilled water with 0.1% H_2O_2. The light microscope was carried out with Lecia DMRE (Leica Microsystems).

Statistics

Values are means ± SE. Statistical comparison of two experimental groups was performed by an unpaired Student's *t*-test. When several groups were compared, this was done by two-way ANOVA followed by post hoc analysis with a *t*-test and Bonferroni correction. *P* values < 0.05 were considered significant.

RESULTS

Effect of BUO on Kidney Weight, Plasma Electrolytes, Creatinine, and Osmolality in Wild-Type and COX-2$^{-/-}$ Mice

There was no significant difference between wild-type and COX-2$^{-/-}$ sham-operated mice with regard to body weight or plasma concentration of sodium and potassium (Table 1). At baseline, the kidney/body weight ratio was lower, and plasma urea, creatinine, and osmolality were elevated significantly in sham-operated COX-2$^{-/-}$ compared with wild-type mice (Table 1). After introduction of BUO in both wild-type and COX-2$^{-/-}$ mice, kidney weight, plasma osmolality, potassium, creatinine, and urea increased significantly compared with sham-operated control mice (Table 1). Apart from increased plasma potassium in COX-2$^{-/-}$ mice, there was no significant difference in the parameters between genotypes after BUO.

Changed COX-2 and COX-1 Expression in Wild-Type Mice in Response to BUO

The abundance of COX-2 mRNA and protein was significantly increased in C+OM tissue homogenates in wild-type mice in response to BUO (Fig. 1, *A* and *B*). In IM homogenates, the COX-2 protein level was increased in BUO wild-type mice (Fig. 1*C*). In COX-2$^{-/-}$ mice, there was no detectable COX-2 mRNA or protein level (Fig. 1, *A*–*C*). Experiments with IM homogenates revealed that the anti-COX-2 antibody (Cayman 160126) labeled a protein of the expected molecular size (~72 kDa). This was completely ablated when the antibody was preincubated with an excess of the immunizing peptide (Fig. 1*D*). To further support the specificity, additional analyses were conducted with different antibodies directed against COX-2 (Cayman 160106 and Abcam ab15191). Both antibodies confirmed the COX-2 result in response to BUO and further corroborate the findings (Fig. 1*D*). Immunohistochemical staining of kidney IM sections revealed that COX-2-immunoreactive protein was localized to the medullary interstitial cells in the obstructed kidney, and there was no detectable labeling in the COX-2$^{-/-}$ mice subjected to BUO (Fig. 1, *E* and *F*). At baseline, mice deficient in COX-2 showed a significant increase in COX-1 protein abundance in both C+OM and IM (Fig. 2, *A* and *B*). In wild-type mice, COX-1 protein abundance increased after BUO in both C+OM and IM compared with sham-operated animals (Fig. 2, *A* and *B*); in C+OM of COX-2$^{-/-}$ mice, COX-1 expression increased further in response to BUO whereas it was unaltered at a high level in the IM (Fig. 2, *A* and *B*).

Effect of BUO on Renal AQP2 Abundance and Localization in Wild-Type and COX-2$^{-/-}$ Mice

In C+OM fraction, total AQP2 mRNA and protein abundance significantly decreased in wild-type BUO-operated mice compared with sham-operated wild-type mice. In BUO-operated COX-2$^{-/-}$ mice, downregulation of total AQP2 was attenuated at both mRNA and protein levels (Fig. 3, *A* and *B*). Immunohistochemistry of cortical sections demonstrated that wild-type mice subjected to BUO showed weaker labeling of AQP2 in the apical plasma membranes in collecting duct principal cells compared with sham-operated wild-type mice. COX-2$^{-/-}$ mice subjected to BUO showed stronger labeling of AQP2 compared with obstructed wild-type mice (Fig. 3, *C*–*F*).

AQP2 mRNA levels in the IM did not differ between sham-operated wild-type and COX-2$^{-/-}$ while it was suppressed below 5% of sham levels following obstruction in both genotypes (Fig. 4*A*). Total AQP2 protein abundances in the IM did not differ between genotypes in sham-operated mice. After BUO induction, AQP2 protein abundances decreased equally in wild-type and COX-2$^{-/-}$ mice compared with sham-operated mice (Fig. 4*B*). However, total AQP2 protein was signif-

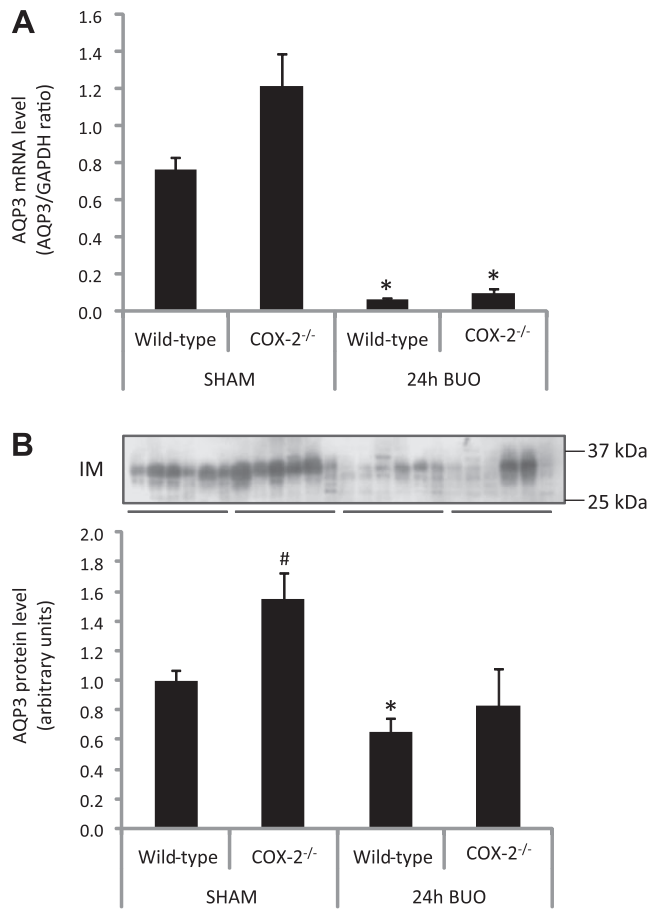

Fig. 6. Effect of BUO on IM regulation of AQP3 in COX-2$^{-/-}$ and wild-type mice. *A*: IM AQP3 mRNA level is significantly decreased in response to BUO in both genotypes. *B*: IM AQP3 protein abundance is significantly decreased in wild-type mice in response to BUO. Furthermore, significant upregulation at baseline is shown in COX-2$^{-/-}$ compared with wild-type mice. *$P < 0.05$ BUO-operated compared with sham-operated mice. #$P < 0.05$ sham-operated wild-type compared with sham-operated COX-2$^{-/-}$ mice.

icantly decreased in COX-2$^{-/-}$ compared with wild-type mice after BUO.

The pAQP2 protein level in C+OM did not differ between genotypes as well as sham-operated control and BUO-operated mice. In the IM, pAQP2 was significantly suppressed in both genotypes after BUO compared with wild-type mice (data not shown).

Effect of BUO on Renal AQP3 Abundance and Localization in Wild-Type and COX-2$^{-/-}$ Mice

AQP3 mRNA levels did not differ between genotypes in C+OM in sham-operated mice (Fig. 5*A*). However, at the protein level AQP3 was increased in the COX-2$^{-/-}$ mice (Fig. 5*B*). Upon obstruction, AQP3 mRNA and protein levels in C+OM decreased significantly in wild-type mice, while deletion of COX-2 rescued the AQP3 protein level and improved the AQP3 mRNA level (Fig. 5, *A* and *B*). Immunohistochemical labeling of kidney sections for AQP3 demonstrated that sham-operated wild-type mice displayed a less marked labeling pattern associated with cortical collecting duct basolateral membranes compared with COX-2$^{-/-}$ mice (Fig. 5, *C* vs. *D*). After obstruction, wild-type mice exhibited labeling close to the detection threshold, while labeling of COX-2$^{-/-}$ kidneys subjected to BUO was indistinguishable from sham-operated COX-2$^{-/-}$ mice (Fig. 5, *E* and *F*).

In the IM, AQP3 mRNA was not different between COX-2$^{-/-}$ and wild-type mice, while at the protein level AQP3 was significantly increased in the sham-operated COX-2$^{-/-}$ mice compared with wild-type. AQP3 mRNA level decreased significantly after BUO in COX-2$^{-/-}$ and wild-type compared with sham-operated mice, while at the protein level AQP3 was only significantly reduced in the wild-type BUO-operated mice (Fig. 6, *A* and *B*).

Effect of BUO on Renal AQP Abundance in Parecoxib-Treated and Control Mice

A last series of experiments tested the effect of a COX-2 inhibitor in sham-operated and BUO wild-type mice. Wild-type mice were treated with a COX-2 inhibitor and then subjected to sham operation or BUO, and changes in COX-1, AQP2, and -3 protein abundances were analyzed.

To examine the effect of the COX-2 inhibitor parecoxib, the cortical COX-2 mRNA level was measured in treated and untreated control mice, which demonstrated threefold increase

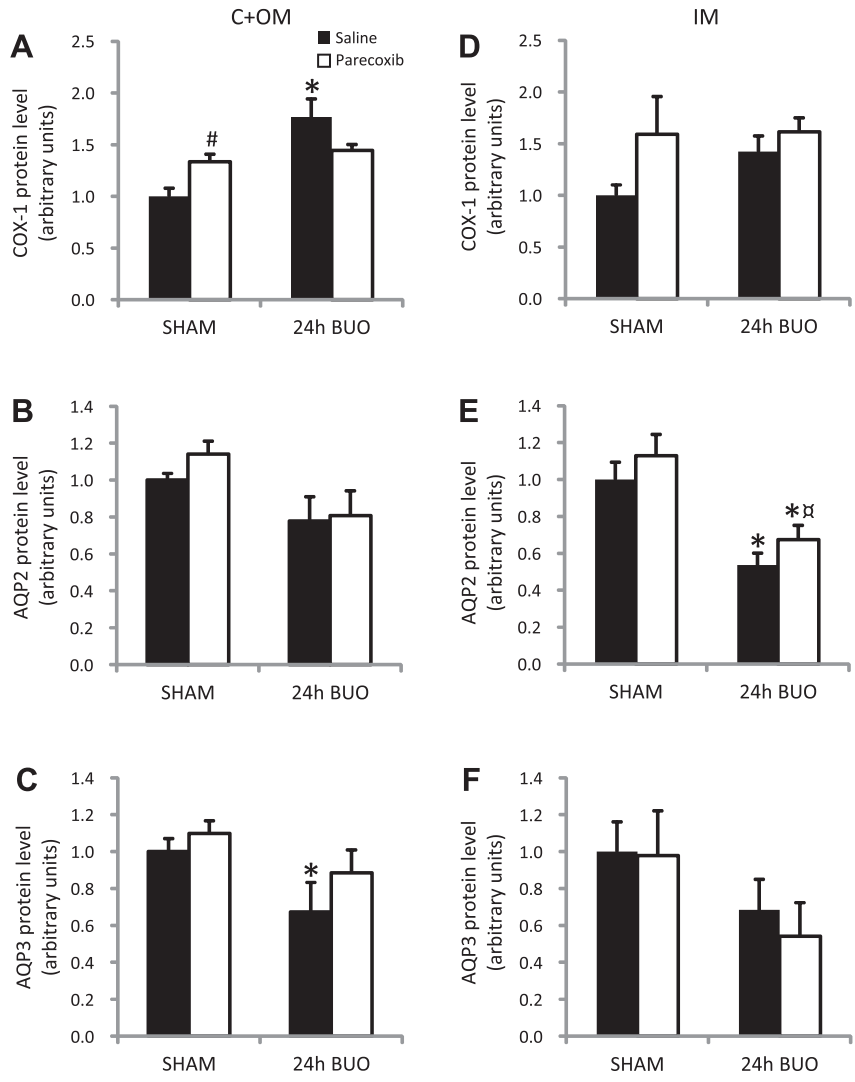

Fig. 7. Effect of 24-h BUO on C+OM and IM AQPs in vehicle- and parecoxib-treated wild-type mice. *A*: COX-1 protein level in C+OM. *B*: AQP2 protein level in C+OM. *C*: AQP3 protein level in C+OM. *D*: COX-1 protein level in IM. *E*: AQP2 protein level in IM. *F*: AQP3 protein level in IM. *$P < 0.05$ BUO-operated compared with sham-operated mice. #$P < 0.05$ sham-operated, vehicle-treated compared with sham-operated, parecoxib-treated mice. ¤$P < 0.05$ BUO-operated, vehicle-treated compared with BUO-operated, parecoxib-treated mice.

in COX-2 expression in response to parecoxib treatment compared with control mice (COX-2/β-actin ratio: 1.03 ± 0.31 vs. 0.31 ± 0.03, $P < 0.05$) (10, 16). The COX-1 protein level was increased in BUO-operated mice compared with sham-operated mice in both C+OM and IM (Fig. 7, *A* and *D*), although it did not reach a significant level in the IM ($P = 0.057$). Parecoxib treatment significantly increased COX-1 protein in C+OM in sham-operated mice. AQP2 protein abundance was not significantly regulated in C+OM in sham-operated control mice, but there was a tendency of upregulation in response to parecoxib (Fig. 7*B*). In BUO-operated mice, there was a tendency toward a downregulation of AQP2 compared with sham-operated mice, although it was not significant. In the IM, AQP2 protein abundance was decreased in response to BUO, and this downregulation was attenuated by administration of parecoxib (Fig. 7*E*). In response to BUO, there was a significant downregulation of pAQP2 in the IM. Treatment with parecoxib increased pAQP2 in C+OM in sham-operated mice (data not shown). AQP3 protein abundance was significantly decreased in BUO-operated compared with sham-operated mice in C+OM (Fig. 7*C*), and a tendency of downregulation in the IM (Fig. 7*F*). Administration of the selective COX-2 inhibitor parecoxib partly attenuated the decreased AQP3 protein level in C+OM after BUO.

Immunohistochemical staining of cortical sections displayed a weaker apical AQP2 labeling in collecting duct principal cells in BUO-operated mice compared with sham-operated mice (Fig. 8, *A* vs. *C*). Cortical labeling of AQP3 showed that vehicle-treated mice subjected to BUO display weaker labeling in the basolateral plasma membranes in collecting duct principal cells compared with sham-operated, vehicle-treated mice (Fig. 8, *E* vs. *G*). Parecoxib-treated, BUO-operated mice exhibited stronger labeling of AQP3 compared with obstructed vehicle-treated mice, indistinguishable from sham-operated, parecoxib-treated mice (Fig. 8, *E–H*).

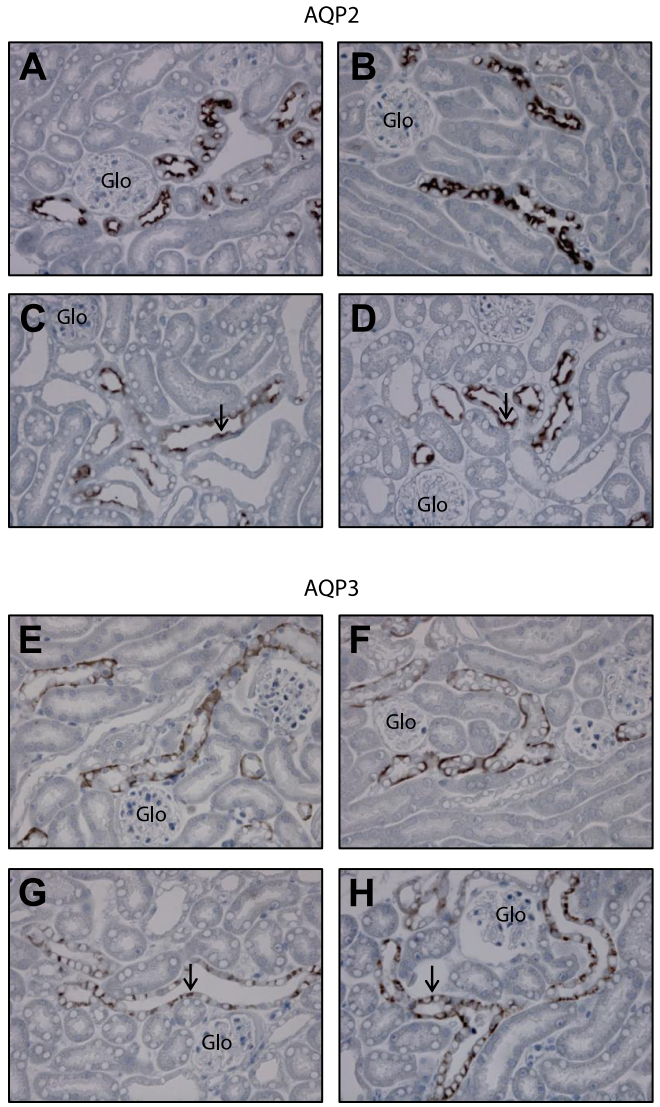

Fig. 8. Cortical immunohistochemical staining of AQPs in vehicle- and parecoxib-treated wild-type mice. *A–D*: cortical immunohistochemical staining of AQP2 showed weaker labeling in BUO-operated, vehicle-treated mice compared with sham-operated mice. *A*: sham-operated, vehicle-treated. *B*: sham-operated, parecoxib-treated. *C*: BUO-operated, vehicle-treated. *D*: BUO-operated, parecoxib-treated. *E–H*: cortical immunohistochemical staining of AQP3 showed stronger labeling in parecoxib-treated, BUO-operated mice compared with vehicle-treated, BUO-operated mice. Panels E–F are as described for *A–D*.

DISCUSSION

The present study shows that BUO in wild-type mice leads to a significant induction of COX-1 and COX-2 protein and downregulation of AQP2 and -3. COX-2 displayed the largest increase after BUO and was associated with renomedullary interstitial cells. C57BL/6 mice with disrupted COX-2 (COX-$2^{-/-}$) were protected from BUO-induced suppression of AQP2 and -3 in C+OM tissue despite compensatory stimulation of COX-1 protein at baseline. This protection of AQP decreased protein levels by disruption of COX-2 was partially recapitulated by administration of a specific COX-2 blocker to wild-type BUO-operated mice. Thus C57BL/6 mice appear as a valid model that reproduces acute downregulation of AQPs after BUO in rats, and the data might indicate that downregulation of AQP2 and AQP3 after release of BUO and subsequent acute polyuria is mediated mainly by COX-2-derived prostaglandins.

A minor difference in rescue of AQPs in the IM between COX-$2^{-/-}$ (absent protection) and parecoxib-treated wild-type (partial protection) mice was detected. This difference is likely caused by upregulated COX-1 in COX-$2^{-/-}$ mice and attenuated COX-1 activity (lower abundance compared with COX-$2^{-/-}$ and partial nonselective inhibition) in wild-type mice treated with parecoxib.

Changed COX-2 and COX-1 Protein Level in COX-$2^{-/-}$ and Wild-Type Mice in Response to BUO

BUO increases cortical and medullary COX-2 compared with sham-operated mice, and this increase is abolished in COX-$2^{-/-}$ mice. Consistent with previous rat studies, the present study shows that COX-2 is increased in renal medullary interstitial cells in response to BUO (16, 18).

As observed recently (19), the present data confirmed that mice deficient in COX-2 display a compensatory upregulation of COX-1 and further showed that COX-1 was stimulated by BUO in the cortex. Thus the mice exhibit a larger sensitivity to BUO with more widespread upregulation of COX in kidney tissue compared with rats, for example, where cortical COX-1

and -2 did not change after BUO (16). This differential regulation of COX-2 expression between mice and rats has been observed in previous studies with a low-salt diet, treatment with a loop diuretic, and an angiotensin-converting enzyme inhibitor in the cortex (27).

Effect of BUO on Plasma Creatinine and Urea in Wild-Type and COX-2$^{-/-}$ Mice

The observation that sham-operated COX-2$^{-/-}$ mice had increased plasma creatinine and urea is consistent with previous studies in COX-2$^{-/-}$ mice, suggesting reduced renal function in the COX-2$^{-/-}$ mouse (19, 20, 29). Wild-type mice with BUO exhibited a significant increase in the plasma concentration of creatinine, urea, potassium, and osmolality compared with sham-operated mice, consistent with impaired renal function and previous findings in rats (13, 16). COX-2$^{-/-}$ mice subjected to BUO showed a significant, further, increase in plasma potassium compared with obstructed wild-type mice. These results suggest that obstructed mice with homogenous deletion of COX-2 experience further reduction in renal function compared with wild-type mice subjected to BUO. COX-2$^{-/-}$ mice have impaired postnatal kidney development. The defect involves cortical dysplasia, diffuse tubular dilation, hypoplastic subcapsular glomeruli, and juxtamedullary nephron hypertrophy (3, 19, 20, 22). In the present study, COX-2$^{-/-}$ mice displayed accumulation of small glomeruli in the subcapsular region, while the tissue displayed no cysts, inflammation, or fibrosis. The cortical dysplasia with fewer functional outer cortical nephrons may account for the observed changes in plasma creatinine and urea. Despite this injury, the mice were considered suitable to test the hypothesis because it relates to a pathophysiological situation where the glomerular filtration rate is reduced experimentally to a minimal level, and because the COX-2$^{-/-}$ mouse exhibits AQP levels that are normal to elevated in the control situation (19). Moreover, the mouse reacts to BUO similarly to the rat with a massive COX-2 induction in the medulla.

Effect of BUO on Renal AQP2 and AQP3 in COX-2$^{-/-}$ and Parecoxib-Treated Wild-Type Mice

The present study documented downregulation of renal AQPs in response to BUO in mice, consistent with several previous rat studies (11, 16). The downregulation of cortical AQP2 and AQP3 in response to BUO was attenuated in COX-2$^{-/-}$ mice, whereas no rescue of AQP2 and AQP3 levels was observed in the IM. Why did COX-2 inhibitor experiments show protection of AQP2 abundance after BUO in the IM, similar to in rats (16), while BUO-induced suppression of AQP2 in the IM of COX-2$^{-/-}$ mice was not attenuated? A likely explanation is the compensatory upregulation of COX-1 by BUO that may supply downstream PGE synthase with substrate even in the absence of functional COX-2. At baseline, there are 25 times higher COX-1 levels in the rat IM compared with the cortex (9). A similar gradient in the mouse with further COX-1 upregulation by BUO in COX-2$^{-/-}$ mice could account for maintained or even increased prostaglandin synthesis. Parecoxib at 5 mg/kg is likely also to have some nonselective inhibitory action on COX-1 (24, 26), which may account for the modest, but significant, attenuation of AQP2 downregulation in the IM after BUO The results further support that in the setting of BUO, COX-2-derived prostanoids either directly or by indirect pressure-related effects suppress transcellular water uptake pathways in the collecting duct. Recent observations show that PGE_2 through EP_2/EP_4 receptors in rare situations (loss-of-function mutations in the vasopressin receptor) may actually preserve collecting duct AQPs and support urine concentrating ability (14). In BUO, there is significant stimulation of prostaglandin synthesis in the renal medulla, while in nephrogenic diabetes insipidus, medullary prostaglandin synthesis is maximally suppressed (8, 18, 28). These very different physiological settings probably account for the different roles associated with prostaglandins to control AQPs.

In summary, the present data show that *1*) the mouse essentially recapitulates the observations from the rat that ureteral obstruction induces renal COX-2 expression and lowers aquaporin abundance and *2*) inhibition of COX-2 activity by targeted disruption or pharmacological blockade in the mouse attenuates obstruction-induced AQP downregulation. The data further support that COX-2-derived prostaglandins contribute to postobstruction diureses and mice with targeted disruption of key signaling molecules could be employed to dissect the cellular events that injure kidney structure and function after ureteral obstruction.

ACKNOWLEDGMENTS

The authors thank Gitte Skou, Gitte Kall, Inger Merete Paulsen, and Line V. Nielsen for expert technical assistance.

GRANTS

The Water and Salt Research Centre at the University of Aarhus is established and supported by the Danish National Research Foundation (Danmarks Grundforskningsfond). The studies were supported by the Commission of the European Union (EU Action Programs), Danish Research Council for Health and Disease, Lundbeck Foundation, Helen and Ejnar Bjørnow Foundation, NOVO Nordisk Foundation, Aase and Ejnar Danielsens Foundation, and AP Møller Foundation.

DISCLOSURES

No conflicts of interest, financial or otherwise, are declared by the authors.

AUTHOR CONTRIBUTIONS

Author contributions: L.N., K.M., B.L.J., J.F., and R.N. provided conception and design of research; L.N., K.M., S.O.T., and R.N. performed experiments; L.N., S.O.T., and R.N. analyzed data; L.N., S.O.T., and R.N. interpreted results of experiments; L.N., B.L.J., J.F., and R.N. prepared figures; L.N., K.M., B.L.J., J.F., and R.N. drafted manuscript; L.N., K.M., S.O.T., B.L.J., J.F., and R.N. edited and revised manuscript; L.N., K.M., S.O.T., B.L.J., J.F., and R.N. approved final version of manuscript.

REFERENCES

1. **Cheng X, Zhang H, Lee HL, Park JM.** Cyclooxygenase-2 inhibitor preserves medullary aquaporin-2 expression and prevents polyuria after ureteral obstruction. *J Urol* 172: 2387–2390, 2004.
2. **Christensen BM, Zelenina M, Aperia A, Nielsen S.** Localization and regulation of PKA-phosphorylated AQP2 in response to V_2-receptor agonist/antagonist treatment. *Am J Physiol Renal Physiol* 278: F29–F42, 2000.
3. **Dinchuk JE, Car BD, Focht RJ, Johnston JJ, Jaffee BD, Covington MB, Contel NR, Eng VM, Collins RJ, Czerniak PM.** Renal abnormalities and an altered inflammatory response in mice lacking cyclooxygenase II. *Nature* 378: 406–409, 1995.
4. **Ecelbarger CA, Terris J, Frindt G, Echevarria M, Marples D, Nielsen S, Knepper MA.** Aquaporin-3 water channel localization and regulation in rat kidney. *Am J Physiol Renal Fluid Electrolyte Physiol* 269: F663–F672, 1995.

5. **Friis UG, Madsen K, Svenningsen P, Hansen PB, Gulaveerasingam A, Jorgensen F, Aalkjaer C, Skott O, Jensen BL.** Hypotonicity-induced Renin exocytosis from juxtaglomerular cells requires aquaporin-1 and cyclooxygenase-2. *J Am Soc Nephrol* 20: 2154–2161, 2009.
6. **Frøkiær J, Marples D, Knepper MA, Nielsen S.** Bilateral ureteral obstruction downregulates expression of vasopressin-sensitive AQP-2 water channel in rat kidney. *Am J Physiol Renal Fluid Electrolyte Physiol* 270: F657–F668, 1996.
7. **Hebert RL, Jacobson HR, Breyer MD.** PGE_2 inhibits AVP-induced water flow in cortical collecting ducts by protein kinase C activation. *Am J Physiol Renal Fluid Electrolyte Physiol* 259: F318–F325, 1990.
8. **Jackson BA.** Renal prostaglandin E2 synthesis in the Brattleboro homozygous diabetes insipidus rat. *Prostaglandins Leukot Med* 22: 101–110, 1986.
9. **Jensen BL, Schmid C, Kurtz A.** Prostaglandins stimulate renin secretion and renin mRNA in mouse renal juxtaglomerular cells. *Am J Physiol Renal Fluid Electrolyte Physiol* 271: F659–F669, 1996.
10. **Klein T, Ullrich V, Pfeilschifter J, Nusing R.** On the induction of cyclooxygenase-2, inducible nitric oxide synthase and soluble phospholipase A2 in rat mesangial cells by a nonsteroidal anti-inflammatory drug: the role of cyclic AMP. *Mol Pharmacol* 53: 385–391, 1998.
11. **Li C, Wang W, Knepper MA, Nielsen S, Frøkiær J.** Downregulation of renal aquaporins in response to unilateral ureteral obstruction. *Am J Physiol Renal Physiol* 284: F1066–F1079, 2003.
12. **Li C, Wang W, Kwon TH, Isikay L, Wen JG, Marples D, Djurhuus JC, Stockwell A, Knepper MA, Nielsen S, Frøkiær J.** Downregulation of AQP1, -2, and -3 after ureteral obstruction is associated with a long-term urine-concentrating defect. *Am J Physiol Renal Physiol* 281: F163–F171, 2001.
13. **Li C, Wang W, Kwon TH, Knepper MA, Nielsen S, Frøkiær J.** Altered expression of major renal Na transporters in rats with bilateral ureteral obstruction and release of obstruction. *Am J Physiol Renal Physiol* 285: F889–F901, 2003.
14. **Li JH, Chou CL, Li B, Gavrilova O, Eisner C, Schnermann J, Anderson SA, Deng CX, Knepper MA, Wess J.** A selective EP4 PGE2 receptor agonist alleviates disease in a new mouse model of X-linked nephrogenic diabetes insipidus. *J Clin Invest* 119: 3115–3126, 2009.
15. **Nielsen J, Kwon TH, Praetorius J, Frøkiær J, Knepper MA, Nielsen S.** Aldosterone increases urine production and decreases apical AQP2 expression in rats with diabetes insipidus. *Am J Physiol Renal Physiol* 290: F438–F449, 2006.
16. **Nørregaard R, Jensen BL, Li C, Wang W, Knepper MA, Nielsen S, Frøkiær J.** COX-2 inhibition prevents downregulation of key renal water and sodium transport proteins in response to bilateral ureteral obstruction. *Am J Physiol Renal Physiol* 289: F322–F333, 2005.
17. **Nørregaard R, Jensen BL, Topcu SO, Diget M, Schweer H, Knepper MA, Nielsen S, Frøkiær J.** COX-2 activity transiently contributes to increased water and NaCl excretion in the polyuric phase after release of ureteral obstruction. *Am J Physiol Renal Physiol* 292: F1322–F1333, 2007.
18. **Nørregaard R, Jensen BL, Topcu SO, Wang G, Schweer H, Nielsen S, Frøkiær J.** Urinary tract obstruction induces transient accumulation of COX-2-derived prostanoids in kidney tissue. *Am J Physiol Regul Integr Comp Physiol* 298: R1017–R1025, 2010.
19. **Nørregaard R, Madsen K, Hansen PB, Bie P, Thavalingam S, Frøkiær J, Jensen BL.** COX-2 disruption leads to increased central vasopressin stores and impaired urine concentrating ability in mice. *Am J Physiol Renal Physiol* 301: F1303–F1313, 2011.
20. **Norwood VF, Morham SG, Smithies O.** Postnatal development and progression of renal dysplasia in cyclooxygenase-2 null mice. *Kidney Int* 58: 2291–2300, 2000.
21. **Olesen ET, Rutzler MR, Moeller HB, Praetorius HA, Fenton RA.** Vasopressin-independent targeting of aquaporin-2 by selective E-prostanoid receptor agonists alleviates nephrogenic diabetes insipidus. *Proc Natl Acad Sci USA* 108: 12949–12954, 2011.
22. **Olliges A, Wimmer S, Nusing RM.** Defects in mouse nephrogenesis induced by selective and non-selective cyclooxygenase-2 inhibitors. *Br J Pharmacol* 163: 927–936, 2011.
23. **Padi SS, Jain NK, Singh S, Kulkarni SK.** Pharmacological profile of parecoxib: a novel, potent injectable selective cyclooxygenase-2 inhibitor. *Eur J Pharmacol* 491: 69–76, 2004.
24. **Riendeau D, Percival MD, Brideau C, Charleson S, Dube D, Ethier D, Falgueyret JP, Friesen RW, Gordon R, Greig G, Guay J, Mancini J, Ouellet M, Wong E, Xu L, Boyce S, Visco D, Girard Y, Prasit P, Zamboni R, Rodger IW, Gresser M, Ford-Hutchinson AW, Young RN, Chan CC.** Etoricoxib (MK-0663): preclinical profile and comparison with other agents that selectively inhibit cyclooxygenase-2. *J Pharmacol Exp Ther* 296: 558–566, 2001.
25. **Sakairi Y, Jacobson HR, Noland TD, Breyer MD.** Luminal prostaglandin E receptors regulate salt and water transport in rabbit cortical collecting duct. *Am J Physiol Renal Fluid Electrolyte Physiol* 269: F257–F265, 1995.
26. **Smith HS, Baird W.** Meloxicam and selective COX-2 inhibitors in the management of pain in the palliative care population. *Am J Hosp Palliat Care* 20: 297–306, 2003.
27. **Wagner C, Vitzthum H, Castrop H, Schumacher K, Bucher M, Albertin S, Coffman TM, Arendshorst WJ, Kurtz A.** Differential regulation of renin and Cox-2 expression in the renal cortex of C57Bl/6 mice. *Pflügers Arch* 447: 214–222, 2003.
28. **Yanagisawa H, Moridaira K, Nodera M, Wada O.** Ureteral obstruction enhances eicosanoid production in cortical and medullary tubules of rat kidneys. *Kidney Blood Press Res* 20: 398–405, 1997.
29. **Yang T, Huang YG, Ye W, Hansen P, Schnermann JB, Briggs JP.** Influence of genetic background and gender on hypertension and renal failure in COX-2-deficient mice. *Am J Physiol Renal Physiol* 288: F1125–F1132, 2005.